Published by Nigerian Society of Physical Sciences. **Hosted by** FLAYOO Publishing House LTD

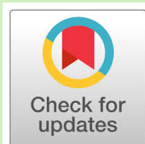

Recent Advances in Natural Sciences

Journal Homepage: https://flayoophl.com/journals/index.php/rans

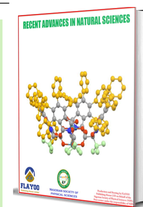

Annealing effect on morphology, surface roughness and structure of thermally evaporated tin oxide thin films

Abideen A. Ibiyemi*, M. A. Ilyas, Jamiu Lawal

Department of Physics, Federal University Oye Ekiti, Nigeria

ARTICLE INFO

Article history:
Received: 07 September 2023
Received in revised form: 26 Oct. 2023
Accepted: 05 November 2023
Available online: 26 November 2023

Keywords: Tin films, Thermal vacuum evaporation, Root mean square

DOI:10.61298/rans.2023.1.2.38

ABSTRACT

SnO_2 thin films were produced utilizing the Thermal Vacuum Evaporation method on quartz substrates. Three samples—FAA, FV-200, and FA-400—were made and labelled. While samples of the FV-200 and FA-400 were annealed at 200 °C and 400 °C, respectively, the as deposited thin film is FAA. The root mean square (RMS) roughness, uniformity, and average roughness of the films were all measured using the atomic force microscope. The film was spherical after being annealed at 400 °C, covering the substrate more uniformly with erratic growth. The as-deposited film exhibits an uneven distribution of grains of varying sizes. The sample showed consistent grain development after being annealed at 200 °C. The root mean square values of samples FAA, FV-200, and FA-400 are 42.2 nm, 41.7 nm, and 112.7 nm. The XRD technique was used to measure the samples' structural characteristics. The as-deposited thin film had two diffraction peaks, the strongest of which could be seen at $2\theta = 300$, or the (200) plane of Sn metal. The thin film was annealed in vacuum at 200 °C and revealed three more peaks, with the strongest peak appearing at $2\theta = 30°$, which is consistent with an enhanced structure of Sn metal thin film. The sample annealed at 400 °C revealed high surface roughness compare to other samples and its films are clearly defined, spherical, and cover the substrate more evenly. Whereas, a mixture of large and small grains with uneven distribution throughout the substrate and poor film homogeneity was reveal by film without heat treatment.

© 2023 The Author(s). Production and Hosting by FLAYOO Publishing House LTD on Behalf of the Nigerian Society of Physical Sciences (NSPS). Peer review under the responsibility of NSPS. This is an open access article under the terms of the Creative Commons Attribution 4.0 International license. Further distribution of this work must maintain attribution to the author(s) and the published article's title, journal citation, and DOI.

1. INTRODUCTION

Metal oxide semiconductors, which are found in the hierarchy of semiconductors and include oxides of zinc, titanium, cuprous oxide, tin, and others, are crucial to all technological applications. Because of its low resistivity and high optical visible spectrum transparency, tin oxide (SnO_2) semiconductors are classified as n-type semiconductors with a wide energy band gap of 3.6 eV [1]. These materials have a wide range of applications in photovoltaic cells, optoelectronics, infrared heat mirrors, low emissive windows, smart windows, transparent electromagnetic shielding, antistatic films, flat panel displays, and photo transistors. It is extremely helpful as a transparent conductive oxide electrode [2] due to its stability in air conditions, mechanical hardness, high temperature resistance, strong carrier mobility [3], and chemical stability.

Thin films, pellets, and thick films of tin oxide are all com-

*Corresponding author: Tel.: +2348062198624
e-mail: abideen.ibiyemi@fuoye.edu.ng (Abideen A. Ibiyemi)

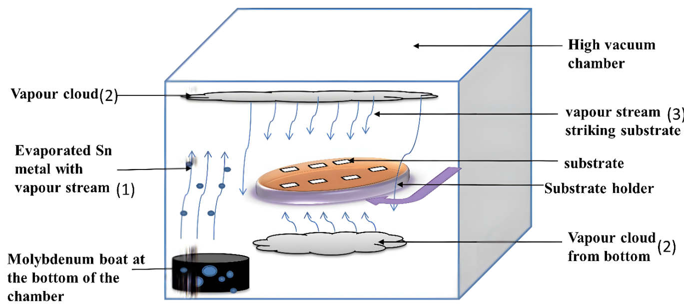

Figure 1. A prototype of the thermal evaporation system thin film deposition process.

mercially available [4]. Tin oxide was a potential replacement for carbon-based materials because of its high capacity storing [5]. The deposition method has a specific impact on properties including morphology, crystal size, thin film thickness, transmittance, absorbance, and thin film uniformity in the context of thin film deposition. For the deposition of SnO_2 thin films, a number of thin film deposition processes have been employed, including the sol-gel technique, spray pyrolysis, magnetron sputtering, chemical vapour deposition, electrostatic spray deposition, and pulse laser deposition [6].

Investigating the effects of the substrate, deposition rate, oxygen pressure, and annealing temperature are further methods utilized to improve the characteristics. It has been reported by Raghupathi *et al.* [7] that thermal evaporation techniques are used to produce films with some non-stoichiometry in their chemical composition because chemical methods exhibit more non-stoichiometry than thermal evaporation because incomplete metallic ion oxidation occurs due to thermal decomposition, which results in the co-existence of SnO_2 phases of various forms in the matrix of the film. Annealing improved electrical conductivity, reduced intrinsic stress, and improved lattice misfit [8, 9]. Therefore, in this work, thermal reactive evaporation, an environmentally benign and controllable method, was used to create thin films of SnO_2. Investigations were conducted on the deposited film's optical transmittance characteristics, thickness uniformity, crystal size, and crystal structure.

2. EXPERIMENTAL PROCEDURE

Quartz substrates were utilized in this study because they were inexpensive, easily accessible, with a high melting point, and did not readily react with chemicals or alter with temperature or moisture. This substrate was ultrasonically cleaned with ethanol and deionized water in order to get a satisfactory deposition, and it was then dried with a Kim swipe. This experiment made use of three substrates. Tin powder is the primary component used in the deposition of tin oxide thin films. A tungsten boat was filled with this powder. Both sides of the prepared substrate sets were left exposed in the substrate holder for coating. The videos were made using a Leybold L560 box with a turbo molecular pump. Before evaporating, the metal powder slowly released gases.

During the evaporation process, the system's base pressure was gradually raised from 5×10^{-4} Pa to 1×10^{-3} Pa. At an evaporation rate of 1 nm/s, the thin films were deposited on the heated substrate [10]. The thickness of the films was managed

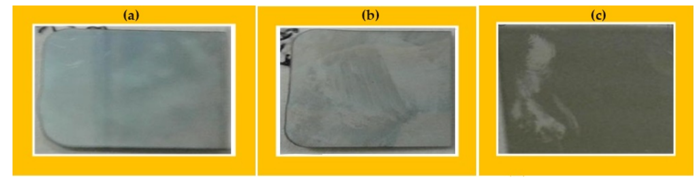

Figure 2. The three as-deposited samples labelled (a) FAA (b) FV-200 (c) FA-400.

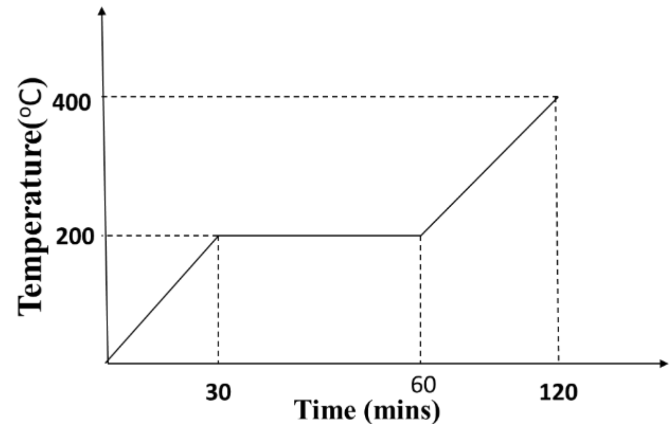

Figure 3. Temperature–time variation profile for the annealing process.

via a quartz crystal thickness monitor. The distance between the substrate holder and the source of the evaporated metal is roughly 40 cm. In order to produce equal deposition, the holder rotates at a steady speed during the deposition procedure. Figure 1 depicts the deposition process, with the numbers (1-3) indicating the various processes in order. As seen in Figure 2, the three samples were labeled FAA, FV-200, and FA-400 for quick identification during the post-deposition procedure.

3. POST-DEPOSITION TREATMENT

The substrate was held at room temperature and at ambient conditions as it was being deposited (FAA). As shown in Figure 3, the temperature was raised to 200 °C for 30 minutes, heated at 200 °C for 30 minutes of dwell time, and then heated to 400 °C for an hour. The FA400 substrate was annealed in air for 400 °C in a gradual process, and the FV-200 thin film was annealed in vacuum at 200 °C. The films were then allowed to cool naturally. Because Sn metal has a melting point of 231.93 °C, this method of annealing is done gradually to prevent the loss of Sn metal.

The optical transmittance spectra of the samples that had been annealed at 400 °C was examined in the wavelength range of 200-1200 nm in order to describe the optical properties of the samples using a UV-VIS Spectrophotometer. Since they did not exhibit transparency from simple eye plucking, other samples were not evaluated. The transmittance values led to the following conclusions.

Equation 1, also known as the Lambert-Beer-Borger rule, which connects the intensity of incident light on the sample with its thickness d, as illustrated in [7], was used to describe the absorption coefficient.

$$I = I_0 \exp(-\alpha d), \quad (1)$$

where I is the transmitted intensity, Io is the intensity of incident light, α is the absorption coefficient and d is the thickness of the sample [11]. The absorption coefficient deduced from equation i is as shown in equation ii which is used to obtain the relation between absorption coefficient and photon energy. Using the transmittance spectrum obtained, the energy band gap of the thin film is determined using the Tauc relation given in equation 3 [12].

$$\alpha = \frac{1}{d} \ln\left(\frac{1}{T}\right), \quad (2)$$

$$\alpha h\nu = h\nu - E_g, \quad (3)$$

where B is the constant with different values of different transition, E_g is the energy gap, hυ is the photon energy. $n = 2$ for the allowed direct transition. Hence $(\alpha h\nu)^2$ is plotted against $h\nu$ for $n = 2$.

CuK radiation with a wavelength of 1.5418 is used in a diffractometer to measure the samples' structural characteristics at 2 θ values between 20° and 80°. The diffraction peaks were used to ascertain the sample's makeup. Due to its excellent resolution and robust analysis software, Atomic Force Microscopy (AFM) is a useful technique for the investigation of thin film surface roughness. Since the precursor grains were produced with varying sizes and spherical in shape on the substrate during the deposition process, the thin film's surface roughness cannot be avoided. The root mean square (RMS) roughness, uniformity, and average roughness of the films were all measured using the atomic force microscope. The three samples used in this analysis were used to demonstrate the impact of annealing on the morphology and surface roughness of tin oxide thin films.

The material used is tin oxide powder heated in a vacuum, tin oxide powder is evaporated in the chamber once it melts and settled on the substrates as thin film. The thin film samples were made to undergo heat treatment at 200 °C and 400 °C. Three samples were prepared, sample labelled with FAA was not subjected to heat treatment, sample labelled with FA-400 was annealed at 400 °C and the sample labelled as FV-200 was annealed at 200 °C. The two samples were annealed to examine the effect of heat treatment on the characteristics of tin oxide thin films.

4. RESULTS AND DISCUSSION

Figure 4 depicts the optical transmittance spectrum of the sample (FA-400), which was annealed at 400 °C in air for four hours. The film transmittance steadily rises at wavelengths between 200 nm and 400 nm. The wavelength region between 1500 nm and 1900 nm shows the maximum transmittance. Due to the thin film's uneven deposition and the existence of porosity, a fluctuating rise was seen in the Uv-Vis region. The material becomes more transparent as light moves into the NIR region, reaching a maximum transmittance of 45%. The low transmittance, when compared to the highest reported transmittance of SnO_2, shows that the Sn metal has not completely oxidized into SnO_2, reducing transparency [13].

The graph in Figure 5 illustrates the correlation between photon energy and the absorption coefficient. The absorption coefficient rises steadily as photon energy rises, suggesting that absorption is highest at high energy, which corresponds to low wavelength, and that reflectance and transmittance are highest at

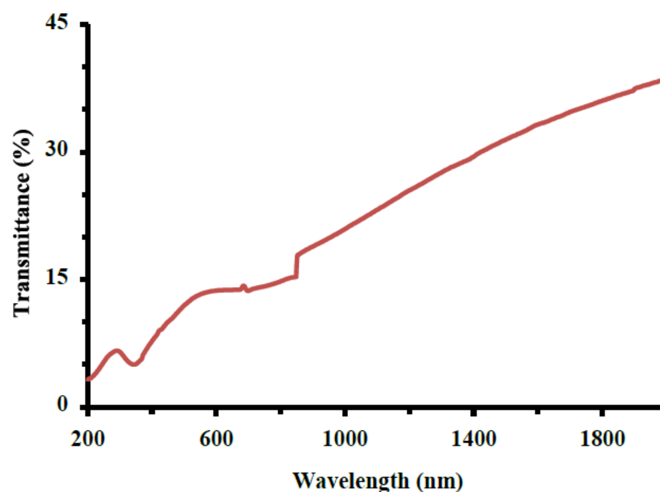

Figure 4. UV-VIS-NIR Transmittance spectrum of the sample annealed at 400^0C in air.

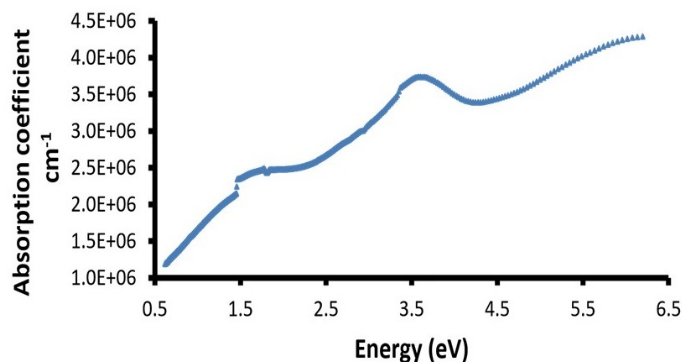

Figure 5. The graph of the absorption coefficient and photon energy relation for the thin film annealed at 400^oC in air.

low energy, which corresponds to high wavelength. This might be caused by SnO_2 having more free electrons than usual. The absorption value varies from 105.5 to 106.0 cm^{-1}.

Figure 6 shows the relation between the $(\alpha h\nu)$ and $h\nu$ with $n = 2$ for allowed direct transition. The band gap is determined by extrapolating the linear portion of the plot to $(\alpha h\nu)^2 = 0$ as shown in the figure. The obtained energy band gap is ~ 3.9 eV which is in agreement with the reported band gap of SnO_2 thin film. The bump noticed along the spectral line is due to the incomplete oxidation of the thin film while annealing.

For the FAA, FV-200, and FA-400 samples, respectively, the AFM images in Figures 7, 8, and 9 were used to examine the root mean square roughness. The films are clearly defined, spherical, and cover the substrate more evenly after being annealed at 400 °C. The thin film's uneven development on the substrate is seen in all samples. The thickness is more uniformly distributed. Figure 7 demonstrates a mixture of large and small grains with uneven distribution throughout the substrate and poor film homogeneity. Because of the vacuum annealing, Figure 8 exhibits a symptom of grain growth in regular form [13]. The smallest grain size, as seen in Figure 9, may be partially caused by the Sn metal. The

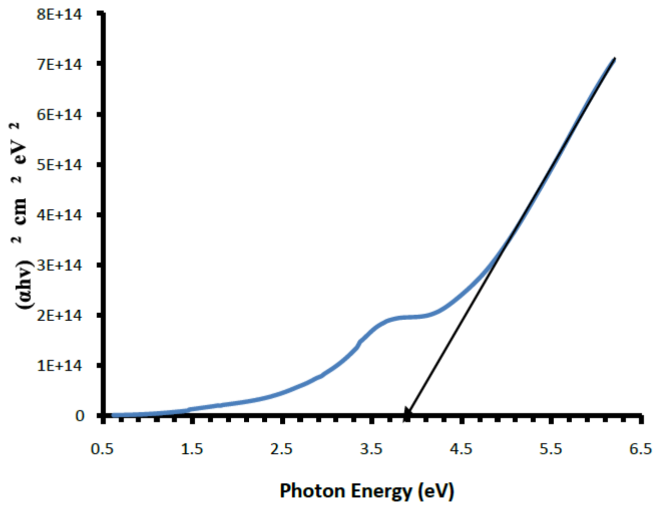

Figure 6. The relation between the $(\alpha h\nu)^2$ and $h\nu$ used in obtaining the band gap.

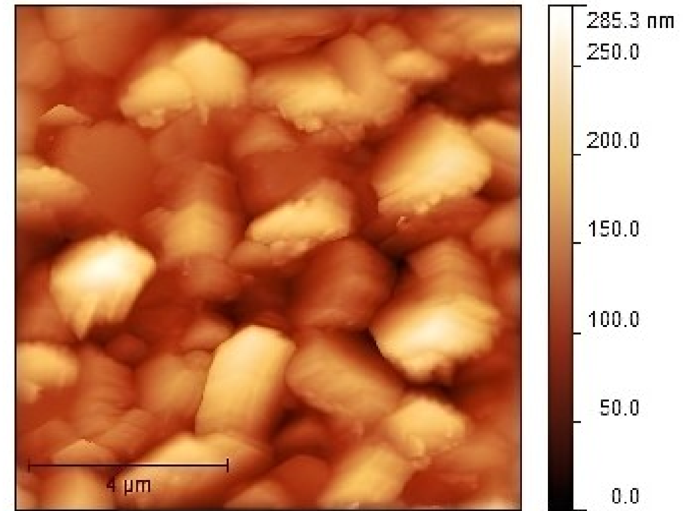

Figure 8. Atomic Force Microscope (AFM) image of the thin film annealed at 200 °C in Vacuum.

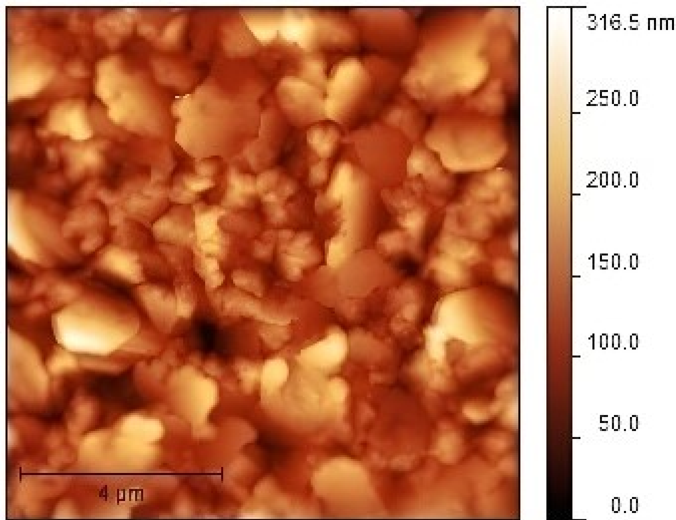

Figure 7. Atomic Force Microscope (AFM) image of as-deposited thin film deposited on quartz substrate.

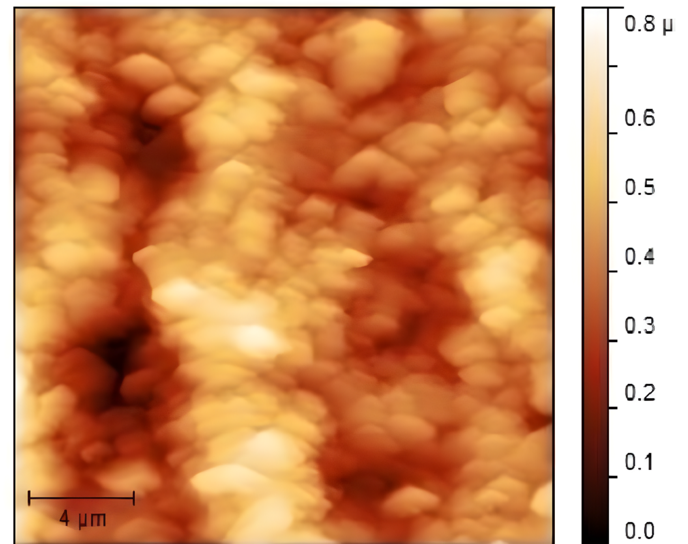

Figure 9. Atomic Force Microscope (AFM) images of SnO_2 of the thin film annealed at 400 °C in air.

surface also exhibits some porosity since there are no coatings in some places, which may be the result of substrate contaminants. This illustrates how annealing affects the development of thin film morphology. High levels of porosity and high levels of surface roughness are present, however they are not very noticeable. The FRR, FV-200, and FA400 samples' respective root mean square values are 42.2 nm, 41.7 nm, and 112.7 nm.

The XRD spectrum of the as-deposited thin film is displayed in Figure 10. The spectra showed two peaks at $2\theta = 30°$ and 64°, with the most powerful peak at $2\theta = 30°$, which corresponds to the 200 plane of Sn metal. This demonstrates that there is only Sn metal present in the thin film that was formed on the substrate and that SnO_2 formation due to the absence of oxygen has not taken place. The XRD spectrum of the thin film that was annealed in vacuum at 200 °C is shown in Figure 11. The most powerful peak was at $2\theta = 30°$, which correlates to an enhanced structure of Sn metal thin film with lack of oxygen. Three more peaks were seen between $2\theta = 39°$ and 64°. The XRD spectrum of the film that was annealed at 400 °C is shown in Figure 12. The spectrum shows a number of peaks, including an intense peak at $2\theta = 30°$ that corresponds to Sn metal that has been deposited, however it is less powerful than other peaks from samples that have been annealed at 200 °C and as-deposited samples. The reflection from the (110) plane accounts for the strongest peak for SnO_2 at $2\theta = 28.9°$. A selected few additional SnO_2 peaks were seen as a result of reflection from the (221), (210), (211), (002), and planes. Insufficient air annealing time or temperature caused Sn metal peaks to form in the spectrum. As a result, the sample has an oxygen deficit and the tin oxide is in the form of (SnO_{2-X}) [11].

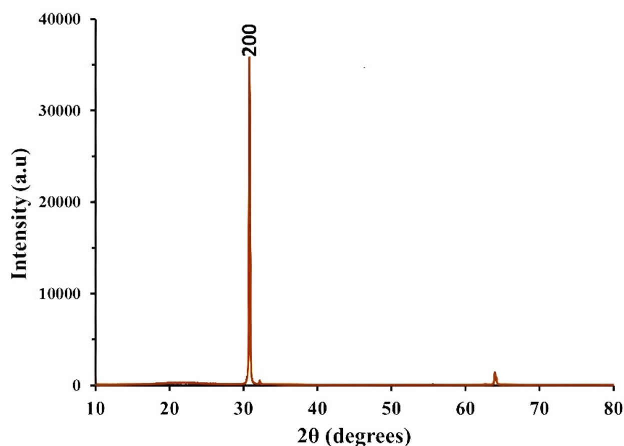

Figure 10. X-ray diffraction pattern of the as-deposited thin film deposited.

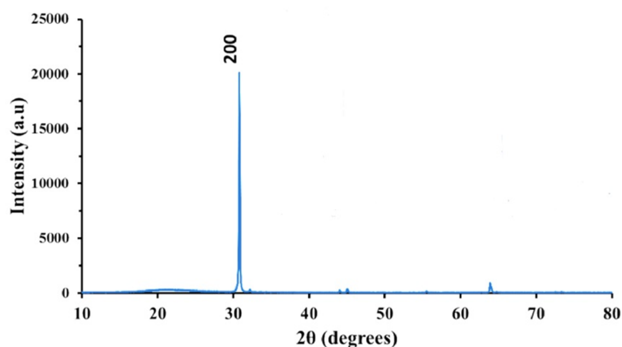

Figure 11. X-ray diffraction pattern of the thin film annealed in vacuum at 200 °C.

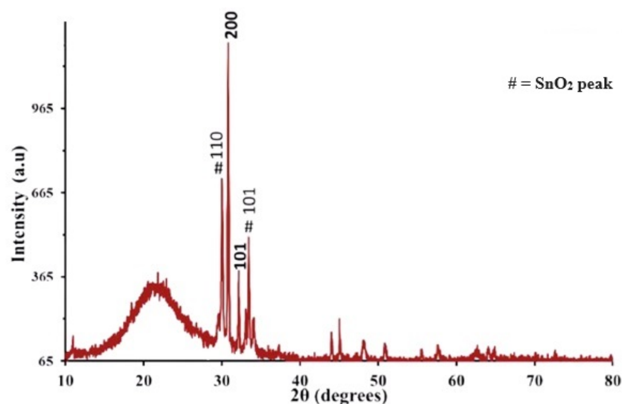

Figure 12. X-ray diffraction patterns of the thin film annealed in air at 400 °C.

5. CONCLUSION.

In this research, effect of heat treatment on the surface roughness and structure of tin oxide thin film was examined. Surface roughness of thermally evaporated tin oxide thin films is clearly affected by annealing, and there are also morphological changes due to the heat treatment of the films. In contrast to other samples, the sample annealed at 400 °C showed a high level of surface roughness, and its films are well-defined, spherical, and cover the substrate more evenly. In contrast, a film without heat treatment revealed a mixture of large and small grains that were dispersed unevenly throughout the substrate and had poor film homogeneity. When the sample is annealed at 200 °C, the roughness is reduced, but increases at 400°C. The X-ray graphs show that the annealing effect also has an impact on the film's structural integrity. The annealing of the film multiplies the diffraction peak. The sample annealed at 400 °C produces multiples diffraction peaks. Using the surface roughness and homogeneity, the thin film samples successfully created using thermal evaporation technology have been assessed structurally and morphologically. Although the claimed band gap has been effectively produced, it is apparent that the SnO_2 film has not been fully formed after annealing in air at 400 °C. This is also demonstrated in the transmittance spectrum, which shows a maximum transmittance of 45%. The annealing condition and temperature must be carefully considered in order to obtain good optical and structural properties from SnO_2 thin films deposited using thermal evaporation technique. Annealing in vacuum does not aid in the formation of tin oxide (SnO_2) but it improves the surface structure and uniformity compared to the as prepared sample.

References

[1] M. F. Al-Kuhaili & S. M. A. Durrani, "Structural and optical properties of dysprosium oxide thin films", Journal of Alloys and Compounds **591** (2014) 234. http://dx.doi.org/10.1016/j.jallcom.2013.12.226.

[2] K. L. Chopra, R. C. Kainthla, D. K. Pnadya, *Physics of thin films*, Academic Press: New York, United State, 1982, pp. 169-235.

[3] N. J. Bhavana, Y. Hyun, S. Y. Sam, "Structural, optical and electrical properties of tin oxide thin films by electrostatic spray deposition", Journal of Electrostatics **71** (2013) 48. https://dx.doi.org/10.1016/j.elstat.2012.11.024.

[4] O. Culha, M. F. Ebeoglugil, I. Birlik, "Synthesis and characterization of semiconductor tin oxide thin films on glass substrate by sol–gel technique", Journal of Science and Technology **51** (2009) 32. https://dx.doi.org/10.1007/s10971-009-1956-8.

[5] K. Manil, K. InKoo, C. Minwoo & W. K. Sok, "Optical properties of 'sputtered indium-tin-oxide thin films", Journal of the Korean Physical Society, **59** (2011) 3280. https://dx.doi.org/10.3938/jkps.59.3280.

[6] G. M. Alonzo-Medina, A. González-González, J. L. Sacedón & A. I. Oliva, "Understanding the thermal annealing process on metallic thin film", IOP Conference Series: Materials Science and Engineering **45** (2013) 012013. https://doi.org/10.1088/1757-899X/45/1/012013.

[7] P. S. Raghupathi, G. Joseph & C. S. Menon, "Effect of substrate temperature on the electrical and optical properties of reactively evaporated tin oxide thin films", Indian Journal of Pure and Applied Physics **43** (2005) 620623. https://nopr.niscpr.res.in/bitstream/123456789/8842/1/IJPAP 2043 288 29 20620-623.pdf.

[8] A. A. Ibiyemi, G. T. Yusuf, A. A. Faremi & K Lateef, "Photophysical Properties of Antimony-Doped Tin Oxide Nanocrystals. FUOYE journal of Pure and Applied Science **2** (2017) 194. http://fjpas.fuoye.edu.ng/index.php/fjpas/article/download/42/37.

[9] G. E Patil, D Kajale, V. B Gaikwad & G. H Jain, "Spray Pyrolysis Deposition of Nanostructured Tin Oxide Thin Films, International Scholarly Research Network (ISRN) Nanotechnology, **2012** (2012) 275872. https://doi.org/10.5402/2012/275872.

[10] J. Priyal & P. Arun, "Parameters influencing the optical properties of SnS thin films", Journal of Semiconductors **34** (2013) 222. https://doi.org/10.1088/1674-4926/34/9/093004.

[11] Z. Yuelan, L. Ying & L. Meilin, "Nanostructured columnar tin oxide thin film electrode for lithium ion batteries", Chemistry of Material **18** (2006) 4643. https://doi.org/10.1021/cm0519378.

[12] M. M. H Rahayi, A. C. Ehsani, M. M. Nkele, M. M. Shahidi & F. I. Ezema, "Synthesis and characterization of tin (IV) oxide thin films", Optical and Quantum Electronics **53** (2021) 222. https://doi.org/10.1007/

s11082-021-02896-x.
[13] H. L. Sang, M. H. David, J. J. Allan & T. L. Randall, "Transparent, Homogeneous Tin Oxide (SnO_2) Thin films containing SnO_2-coated gold nanoparticles", Chemistry of Material **25** (2013) 4697. https://dx.doi.org/10.1021/cm402098n.